# Dynamin 2 along with microRNA-199a reciprocally regulate hypoxia-inducible factors and ovarian cancer metastasis

Hemant P. Joshi[a], Indira V. Subramanian[a,b], Erica K. Schnettler[a], Goutam Ghosh[a], Rajesha Rupaimoole[c], Colleen Evans[b], Manju Saluja[a], Yawu Jing[a], Ivan Cristina[d], Sabita Roy[a,e], Yan Zeng[a], Vijay H. Shah[f], Anil K. Sood[c,d], and Sundaram Ramakrishnan[a,b,g,1]

Departments of [a]Pharmacology, [b]Obstetrics and Gynecology, and [e]Surgery, and [g]Masonic Cancer Center, University of Minnesota, Minneapolis, MN 55455; [c]Gynecologic Oncology and Reproductive Medicine, Cell Biology, and [d]Center for RNA Interference and Non-Coding RNAs, The University of Texas MD Anderson Cancer Center, Houston, TX 77030; and [f]Gastroenterology Research Unit, Department of Internal Medicine, Mayo Clinic, Rochester, MN 55905

Edited by Gregg L. Semenza, Johns Hopkins University School of Medicine, Baltimore, MD, and approved February 20, 2014 (received for review September 18, 2013)

**Hypoxia-driven changes in the tumor microenvironment facilitate cancer metastasis. In the present study, we investigated the regulatory cross talk between endocytic pathway, hypoxia, and tumor metastasis. Dynamin 2 (DNM2), a GTPase, is a critical mediator of endocytosis. Hypoxia decreased the levels of DNM2. DNM2 promoter has multiple hypoxia-inducible factor (HIF)-binding sites and genetic deletion of them relieved hypoxia-induced transcriptional suppression. Interestingly, DNM2 reciprocally regulated HIF. Inhibition of DNM2 GTPase activity and dominant-negative mutant of DNM2 showed a functional role for DNM2 in regulating HIF. Furthermore, the opposite strand of *DNM2* gene encodes miR-199a, which is similarly reduced in cancer cells under hypoxia. miR-199a targets the 3′-UTR of HIF-1α and HIF-2α. Decreased miR-199a expression in hypoxia increased HIF levels. Exogenous expression of miR-199a decreased HIF, cell migration, and metastasis of ovarian cancer cells. miR-199a–mediated changes in HIF levels affected expression of the matrix-remodeling enzyme, lysyloxidase (LOX). LOX levels negatively correlated with progression-free survival in ovarian cancer patients. These results demonstrate a regulatory relationship between DNM2, miR-199a, and HIF, with implications in cancer metastasis.**

microRNA | iron regulation

Epithelial ovarian cancer (EOC) is the leading cause of death among the gynecological malignancies (1). Ascites development and peritoneal metastasis are unique features of ovarian cancer progression. Gas analyses of ovarian cancer ascites show about 2.5% dissolved oxygen content, whereas the blood oxygen content ranges between 15% and 23% (2). Hypoxic areas are common in tumor microenvironment as increased metabolic demands of rapidly proliferating cells outpace oxygen availability. Sustained exposure to hypoxia spurs cells to reorganize cellular processes, and energy-consuming functions, such as endocytosis, are suppressed (3, 4). Hypoxia-inducible factor-1α and hypoxia-inducible factor-2α (HIF-1α/HIF-2α) are principal coordinators of these responses. HIF-1α/HIF-2α are stabilized in hypoxia and associate with hypoxia-inducible factor-1β (HIF-1β) to form heterodimeric transcription factors and induce the expression of target genes (5, 6). HIF-1–mediated expression of lysyloxidase (LOX) cross-links collagens and induces cell migration (7). Epithelial ovarian cancer cells (EOCCs) that have adapted to hypoxia by activating HIF-1 disseminate from primary ovarian tumors and exfoliate into the peritoneal cavity. HIF-1 significantly enhances gene signatures associated with tissue remodeling, the morbidity and mortality associated with EOC (8, 9).

Regulation of HIF-1 is a key step in the hypoxic response with profound implications for EOC metastasis. Under normoxia, HIF-1α is hydroxylated within its oxygen-dependent degradation domain (ODDD) by prolylhydroxylases (PHDs). This reaction is an oxygen-, iron-, 2-oxoglutarate and ascorbate-dependent process. Hydroxylated HIF-1α is recognized and bound by a complex that recruits ubiquitin ligases for proteasomal degradation. In hypoxia, however, low oxygen levels impair PHD hydroxylase activity and HIF-1α is stabilized (5). In this study, we show reciprocal regulations between Dynamin 2 (DNM2), a mediator of endocytosis and HIF. DNM2 is down-regulated in hypoxia via HIF-1α, whereas inhibition of DNM stabilizes HIF-1α. Similarly, DNM2 derived miR-199a from the opposite strand (*DNM2os*) is down-regulated in hypoxia, and targets the 3′-UTR of HIF-1α and HIF-2α. EOCCs overexpressing miR-199a show a distinct phenotype with defects in LOX expression, cell migration, and metastasis. In vivo metastasis and tumor growth of EOC overexpressing miR-199a was significantly inhibited compared with control cells. Together, these studies identify a pathway involving DNM2 and miR-199a regulating HIF, metastasis, and tumor growth in EOC.

## Results

**Hypoxia and HIF-1 Down-Regulate Dynamin 2 in EOCCs.** Hypoxia activates expression of receptor tyrosine kinases (RTKs) and prolongation of their signaling by down-regulating receptor-

### Significance

Tumor cells adapt to hypoxia by modulating energy production and utilization. Endocytosis is an energy-consuming process that is suppressed during hypoxia. Our studies show that Dynamin 2 (DNM2), a key component of endocytic machinery, is transcriptionally suppressed by HIF-1. Genetic and pharmacological inactivation of DNM2 stabilized HIF-1α and HIF-2α. Furthermore, miR-199a, which is encoded from the opposite strand of *DNM2*, exerts reciprocal negative regulation upon HIF-1α and HIF-2α. Overexpression of miR-199a decreased HIF-1α and HIF-2α, cell migration, and metastasis. These findings establish a regulatory loop between endocytic pathway and hypoxic response in tumor cells.

Author contributions: A.K.S. and S. Ramakrishnan designed research; H.P.J., I.V.S., E.K.S., G.G., R.R., C.E., M.S., Y.J., Y.Z., and S. Ramakrishnan performed research; R.R., I.C., S. Roy, and V.H.S. contributed new reagents/analytic tools; H.P.J., I.V.S., E.K.S., G.G., I.C., S. Roy, Y.Z., and A.K.S. analyzed data; H.P.J. participated as part of his MD/PhD thesis; and H.P.J., V.H.S., and S. Ramakrishnan wrote the paper.

The authors declare no conflict of interest.

This article is a PNAS Direct Submission.

Data deposition: The microarray data reported in this paper have been deposited in the Gene Expression Omnibus (GEO) database, www.ncbi.nlm.nih.gov/geo (accession no. GSE32313).

[1]To whom correspondence should be addressed. E-mail: sunda001@umn.edu.

This article contains supporting information online at www.pnas.org/lookup/suppl/doi:10.1073/pnas.1317242111/-/DCSupplemental.

mediated endocytosis . Because DNM2, a ubiquitously expressed large GTPase, plays a crucial role in endocytosis, we investigated whether DNM2 expression is modulated during hypoxia. Our studies show that hypoxia inhibits DNM2 expression in ovarian (Fig. 1 *A* and *B*), breast, and pancreatic cancer cell lines (Fig. S1). Transcriptional down-regulation of *DNM2* under hypoxia was further confirmed by transfecting EOCCs with a luciferase reporter construct. *DNM2* promoter-driven expression of luciferase was inhibited when tumor cells were cultured in hypoxia (Fig. 1*C*). Knockdown of HIF-1α reversed suppression of *DNM2* promoter in hypoxia (Fig. 1*D*). The *DNM2* promoter has five HIF-binding sites (HRE 1–5). Mutation of HRE2 reversed hypoxia-induced suppression of *DNM2* promoter (Fig. 1*E*). ChIP analyses showed increased levels of HIF-1 in *DNM2* promoter (HRE sites 1–3) in hypoxia (Fig. 1*F*). To further confirm the role of HIF-1 in the regulation of *DNM2*, we used HIF-1α knockout mouse embryonic fibroblasts (MEFs). HIF-1α gene deletion abolished the down-regulation of *DNM2* transcripts under hypoxia. Wild-type MEFs showed a 60% reduction in *DNM2* transcript levels under hypoxia (Fig. 1*G*). From these studies, we conclude that DNM2 levels are transcriptionally down-regulated under hypoxia by HIF-1.

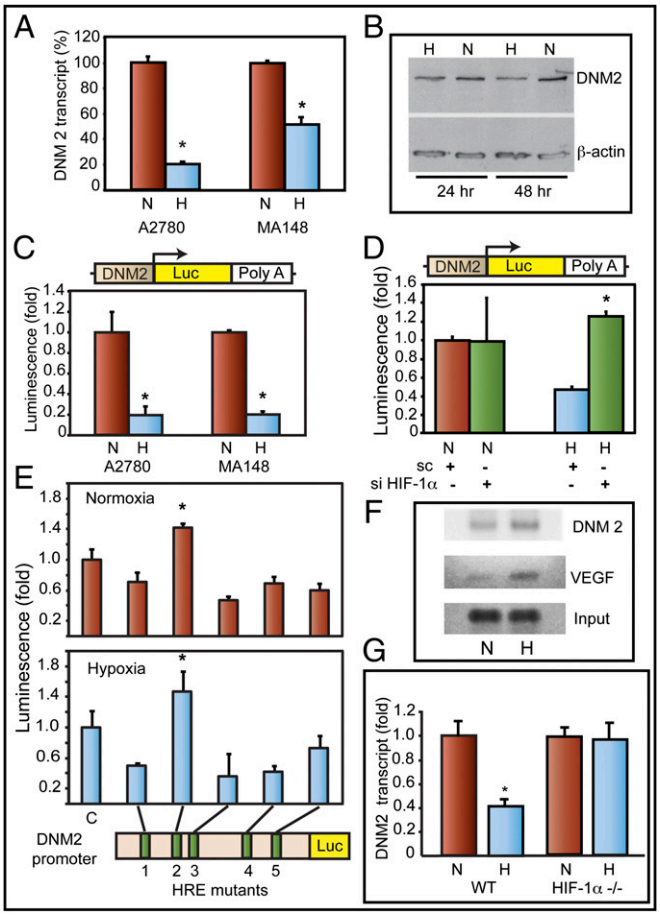


**Fig. 1.** DNM2 is down-regulated in hypoxia in EOCC. (*A*) *DNM2* transcript levels [quantitative PCR (qPCR)] in normoxia (N) or hypoxia (H) are shown. (*B*) Western blot of DNM2. (*C*) (*Upper*) *DNM2* promoter (−1,000)-luciferase reporter construct. (*Lower*) *DNM2* promoter-luciferase expression in normoxia (N) or hypoxia (H). (*D*) HIF-1α knockdown by siRNA rescues *DNM2* promoter activity. (*E*) HRE sites 1 through 5 in *DNM2* promoter were deleted individually. Relative changes in *DNM2* promoter activity were determined by luciferase activity. (*F*) ChIP analyses show HIF-1 binding to HRE sites 1–3 in *DNM2* promoter. HIF-1 binding to *VEGFA* promoter was used as a positive control. (*G*) MEFs from wild-type (WT) and knockout (HIF-1$\alpha^{-/-}$) mice were grown either in normoxia (N) or hypoxia (H). *DNM2* transcript levels were determined by qPCR. Transcript levels in normoxia were considered as 1.0. Values represent mean of transcript levels from three independent cultures.

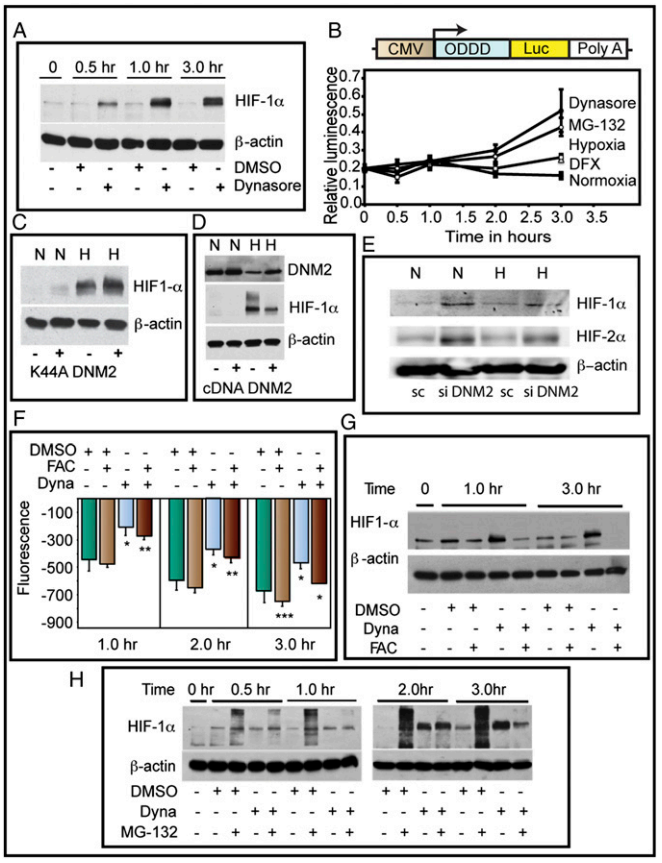


**Fig. 2.** Reciprocal relationship between DNM and HIF-1α. (*A*) Inhibition of Dynamin rapidly stabilizes HIF-1α. Representative Western blot of HIF-1α is shown. (*B*) Dynamin inhibition increases ODDD-HIF-1α-luc fusion protein. (*C*) Dominant-negative DNM (K44A-DNM2) rescued DNM-mediated down-regulation of HIF-1α in hypoxia. Western blot for HIF-1α is shown. Normoxia (N; lanes 1 and 2), hypoxia (H; lanes 3 and 4). (*D*) DNM2 overexpression inhibits HIF-1α. (*E*) DNM2 knockdown increases HIF-1α and HIF-2 α levels (representative Western blot). (*F*) Iron levels were indirectly measured by quenching of calcein-AM fluorescence. (*G*) Stabilization of HIF-1α by Dynamin inhibition is reversed by FAC treatment (representative Western blot). (*H*) Dynamin inhibition blocks polyubiquitination of HIF-1α. Proteasome inhibitor, MG132, was used to block degradation of HIF-1α. Dyna, Dynasore; Sc, scrambled control.

**Dynamin 2 Reciprocally Regulates HIF-1α.** Inhibition of DNM2 activity by Dynasore, a dynamin-specific GTPase inhibitor, increased HIF-1α in normoxia (Fig. 2*A*). Using a reporter construct composed of ODDD of HIF-1α fused to firefly luciferase, we validated the functional significance of DNM2 inhibition (Fig. 2*B*). We then used a genetic approach to validate the pharmacologic inhibition of DNM2. Exogenous expression of K44A-DNM2, a GTPase-dead, dominant-negative mutant, attenuated DNM2 effects on HIF-1α (Fig. 2*C*). DNM2 overexpression conversely reduced the HIF-1α levels (Fig. 2*D*). Furthermore, siRNA mediated knockdown of DNM2 increased the levels of HIF-1α both in normoxia and hypoxia (Fig. 2*E*). Because DNM2 inhibition can affect endocytosis and as a consequence transferrin-mediated iron uptake, we determined intracellular iron levels using calcein-AM. Dynasore treatment reduced iron levels as reflected by

a decrease in fluorescence quenching (Fig. 2*F*). We next delivered iron via DNM2-independent mechanism using ferric ammonium citrate (FAC). FAC increased the intracellular iron pool and reversed DNM2 effects on HIF (Fig. 2*G*). Further studies showed that Dynasore inhibited HIF-1α polyubiquitination (Fig. 2*H*). These data demonstrate that DNM2 controls HIF-1α levels via an iron-dependent mechanism, complementing the reciprocal, negative regulatory effect of HIF-1α on DNM2 expression.

**Micro-RNA Arising from *DNM2* Targets HIF-1α and HIF-2α.** We then investigated whether micro-RNA arising from *DNM2os* could be involved in feedback regulation of HIF. A custom microarray was used (10). The levels of several miRNAs were altered in hypoxic EOCCs (Fig. 3*A*; National Center for Biotechnology Information Gene Expression Omnibus database accession no. GSE32313). miR-199a arising from *DNM2os* was down-regulated under hypoxia. Bioinformatics predicted that the miR-199a-5p targets the HIF-1α (position 31) and HIF-2α (position 2,005) 3′-UTR. This prediction led us to further investigate the role of miR-199a. miR-199a-5p was down-regulated under hypoxia in three EOCC lines (Fig. 3*B*) and breast and pancreatic cancer cell lines (Fig. S1*A*). Hypoxia decreased both the precursor and mature levels of miR-199a-5p (Fig. S1*B*). Different isoforms of miR-199 arise from *DNM* genes. Micro-RNA-199b is encoded from the opposite strand of *DNM1*, and miR-199a1 and miR-199a2 are from *DNM2* and *DNM3*, respectively. Both miR-199a-5p and miR-199b-5p have identical seed sequence and can potentially target the same transcripts. miR-199b levels, however, did not change in hypoxia. miR-199a1 and miR-199a2 are identical except for a single nucleotide. miR-199a2, however, is coexpressed in a single transcript along with miR-214. Array results (Fig. 3*A*) did not show a decrease in miR-214 levels. These results suggest that the decrease seen in miR-199a is primarily due to changes in *DNM2os*-derived miR-199a1. Ct values suggest that miR-199a1-5p is relatively abundant (Ct 24.02) compared with miR-199b (Ct 25.62) in A2780 cells. Similarly, OVCAR3 and MA148 cells showed higher abundance of miR-199a compared with miR-199b (Ct values 25.32 vs. 26.58; 22.88 vs. 25.9, respectively). Ovarian cancer cells showed higher levels of miR-199a-3p compared with miR-199a-5p (Fig. 3*A*). Because miR-199a-5p is relatively abundant than miR-199b-5p and down-regulated in hypoxia, we focused our further studies on miR-199a-5p.

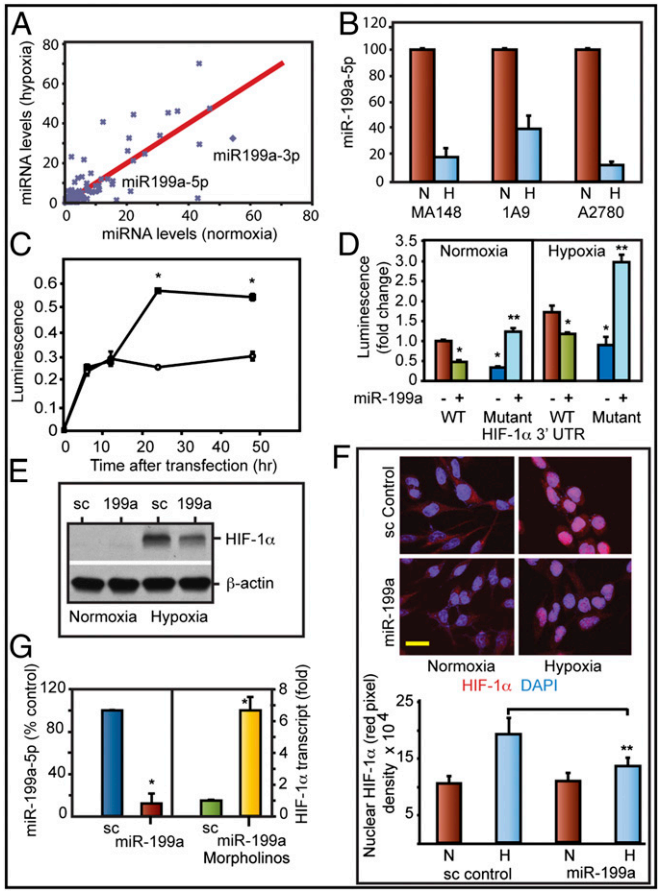


**Fig. 3.** Overexpression of miR-199a targets HIF1α. (*A*) Custom micro-RNA array was used to determine changes in miR expression. (*B*) miR-199a-5p levels (qPCR) in normoxia (N) or hypoxia (H). Values represent mean ± SD from three independent experiments. $*P < 0.05$. (*C*) Luciferase- HIF-1α 3′-UTR (Luc-HIF-1α 3′-UTR) was used as reporter in normoxia (○) or hypoxia (●). (*D*) Luc-HIF1α 3′-UTR and mutant HIF-1α 3′-UTR (seed sequence deletion) were used to determine miR-199a targeting. (*E*) Western blot shows inhibition of HIF-1α levels by miR-199a duplex. (*F*) Confocal images of HIF-1α nuclear translocation. HIF-1α (red) and nuclei (DAPI; blue). (Scale bar: 10 μm.) Histogram shows mean density of red pixel (HIF-1α)/nuclei. (*G*) Relative levels of miR-199a-5p (*Left*) and HIF-1α transcript (*Right*) in A2780 cells after treatment with control morpholino or miR-199a–specific morpholinos. Values represent mean ± SD from three independent determinations. $*P < 0.05$. $**P < 0.001$.

To evaluate whether HIF-1α expression is regulated by a miRNA-dependent mechanism, we used a luciferase cDNA fused to HIF-1α 3′-UTR. A2780 cells transfected with this Luc-HIF-1α-3′-UTR showed higher levels of luciferase activity in hypoxia compared with normoxia (Fig. 3*C*). miR-199a duplex transfection increased the levels of miR-199a severalfold (Fig. S2) and suppressed 3′-UTR reporter activity (Fig. 3*D*). Deletion of target seed sequences in the 3′-UTR of HIF-1α abrogated miR-199a–mediated suppression (Fig. 3*D*). miR-199a duplex (Fig. S3) reduced HIF-1α levels (Fig. 3*E*). miR-199a transfection inhibited nuclear translocation of HIF-1α under hypoxia (Fig. 3*F*). Finally, suppressing endogenous miR-199a expression using a morpholino designed to specifically interfere with miR-199a synthesis and maturation increased HIF-1α transcript levels (Fig. 3*G*).

In addition to HIF-1α, 3′-UTR of HIF-2α also has a target site for miR-199a. Secondary structure prediction analyses (RNAfold) suggest that 3′-UTR of HIF-1α and HIF-2α are different. However, the miR-199a target sequences folds back to the proximal end of 3′-UTR (Fig. 4*A*). miR-199a duplex transfection decreased HIF-2α transcript levels significantly both in normoxia and hypoxia (Fig. 4*B*). Western blots showed a decrease of 23% in HIF-2α levels in hypoxia (Fig. 4*C*). Blots were also reprobed for HIF-1β. Hypoxia increased HIF-1β levels by 17% compared with normoxia. miR-199a duplex transfection did not change HIF-1β levels under hypoxia. In normoxia, however, there was a 13% decrease in HIF-1β in miR-199a–transfected cells. A2780 cells were then infected with a lentivirus construct to express either GFP or miR-199a and GFP. Confocal studies showed that hypoxia-induced nuclear accumulation of HIF-2α was significantly inhibited by miR-199a expression (Fig. 4*D*). The histogram shows quantification of HIF-2α translocated into nuclei. These studies suggest that miR-199a targets both HIF-1α and HIF-2α.

**miR-199a Inhibits Migration of EOC Cells.** Recent studies have demonstrated a direct correlation between increased mortality in ovarian cancer patients with HIF-1 target gene signatures related to matrix remodeling (9). Therefore, we next investigated the effect of miR-199a on ovarian cancer cell proliferation and migration. Ovarian cancer cells were stably transfected with a lentivirus construct to overexpress miR-199a (Fig. S3). miR-199a overexpression reduced HIF-1α (Fig. S4*A*). miR-199a transduction did not affect either cell proliferation or clonogenic growth (Figs. S5 and S6). However, miR-199–transduced cells

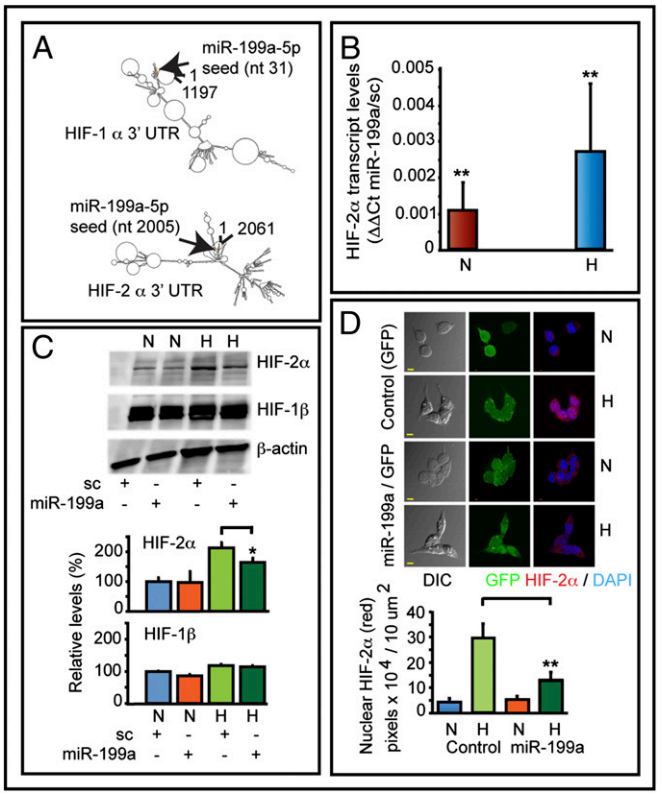


**Fig. 4.** Effect of miR-199a on HIF-2α. (*A*) RNA-fold secondary structure prediction analyses of HIF-1α and HIF-2α 3′-UTR. (*B*) Transfection of miR-199a decreased HIF-2α transcript levels as determined by qPCR. Data show ΔΔCt values comparing transcript levels between miR-199a–transfected and control duplex (sc) transfected cells. Values represent three independent transfections. (*C*) Representative Western blots of HIF-2α and HIF-1β of control and miR-199a duplex transfected cells are shown. (*D*) Confocal images show hypoxia-induced nuclear translocation of HIF-2α was inhibited by miR-199a. A2780 cells were infected with a lentivirus construct to express either GFP alone or coexpress miR-199a and GFP. Histogram shows quantification of red pixel (HIF-2α) localized to 10 $\mu m^2$ of nuclei. (Scale bars: 10 μm.)

showed significantly reduced migration both in normoxia and hypoxia in scratch wound assays (Fig. 5 *A* and *B*). Real-time chemotactic cell migration assays also showed reduced migration of miR-199a–overexpressing cells (Fig. 5*C*). Then we studied the effect of a nondegradable form of HIF-1α mutant on reversing the effect of miR-199a. P-to-A mutation in the ODDD domain of HIF-1α makes it resistant to proteasomal degradation and miR-based regulation due to lack of 3′-UTR. P-to-A HIF-1α mutant mitigated the inhibitory effects of miR-199a on cell migration (Fig. 5 *D* and *E*). These findings were corroborated in real-time cell migration assays (Fig. 5*F*). These data suggest that miR-199a affects EOC cell migration through inhibition of HIF-1α.

**miR-199a Inhibits Peritoneal Seeding and Growth of Ovarian Tumors.** Intraperitoneal injection of A2780-199 cells showed markedly decreased seeding of the ovaries, fallopian tubes, uterus, and gastrointestinal tract compared with animals injected with A2780-GFP cells (Fig. 6 *A* and *B*). These findings were further confirmed in a therapeutic intervention model. A2780-GFP or A2780-199 tumors were established in athymic mice and then treated with carboplatin. A2780-199 tumors were more sensitive to carboplatin than A2780-GFP tumors (Fig. 6 *C* and *D*). These findings suggest that miR-199a impairs EOC seeding of the peritoneum, and carboplatin treatment additively suppresses tumor growth in vivo. miR-199a–mediated changes in tumor burden and response to carboplatin were reflected in reduced vascularization and increased tumor necrosis (Fig. S7 *A*–*E*).

**miR-199a Inhibits ECM Remodeling.** Because A2780-199 cells showed reduced seeding of peritoneum, we investigated whether miR-199a affects HIF-1–mediated changes in matrix remodeling. LOX is a critical mediator of cell attachment to extracellular matrix. LOX cross-links collagens and is induced by HIF-1α. Moreover, LOX affects tumor cell migration and metastasis (7, 11). miR-199a transfection abrogated LOX expression under hypoxia (Fig. 6*E*). Additionally, miR-199a reduced VEGF and EPO transcripts (Fig. S4 *B* and *C*). miR-199a expression also significantly perturbed cell attachment to type I collagen (Fig. 6*F*).

Collagen fibrils, produced by LOX, provide linear tracks for cell migration. Hypoxia-induced EOCC migration was significantly impaired by LOX inhibitor, β-aminoproprionitrile (β-APN) (Fig. 6*G*). We next determined LOX levels in A2780-GFP and A2780-199 tumors. LOX expression was reduced in A2780-199 tumors. Moreover, reduced LOX expression correlated with lower levels of cross-linked fibrillar collagen in A2780-199 tumor sections (Fig. 6*H*). Our findings demonstrate that miR-199a suppresses LOX

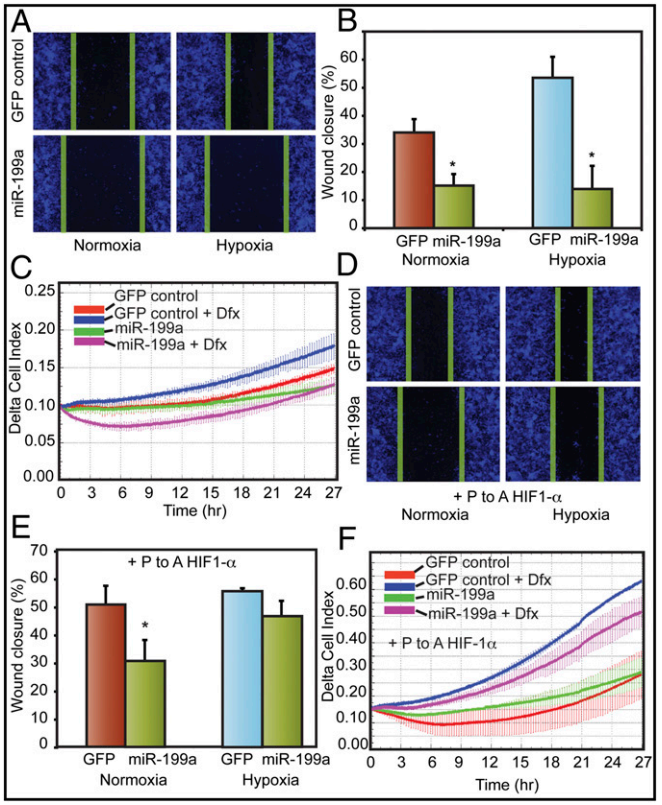


**Fig. 5.** miR-199a stably expressed in EOCC suppresses cell migration in vitro. (*A*) Representative images of scratch/wound assays of A2780 cells expressing GFP or miR-199a/GFP lentivirus are shown. The green lines indicate wound edge (migration). (*B*) Migration distances were measured from six wells per group, and the average percentage of wound closure was calculated. (*C*) Real-time migration of A2780 cells expressing GFP or miR-199a/GFP in the presence and absence of hypoxia mimetic DFX. Delta cell index indicates electrical impedance measurements. (*D*) miR-199a effects on cell migration were mitigated by overexpressing nondegradable form of HIF-1α lacking 3′-UTR. Cells transfected with P-to-A HIF-1α, exposed to normoxia or hypoxia, are shown. (*E*) Quantification of scratch/wound assay described in *D*. (*F*) Real-time migration of A2780 GFP or miR-199a/GFP cells transfected with P-to-A HIF-1α. Values represent mean ± SD. $*P < 0.05$.

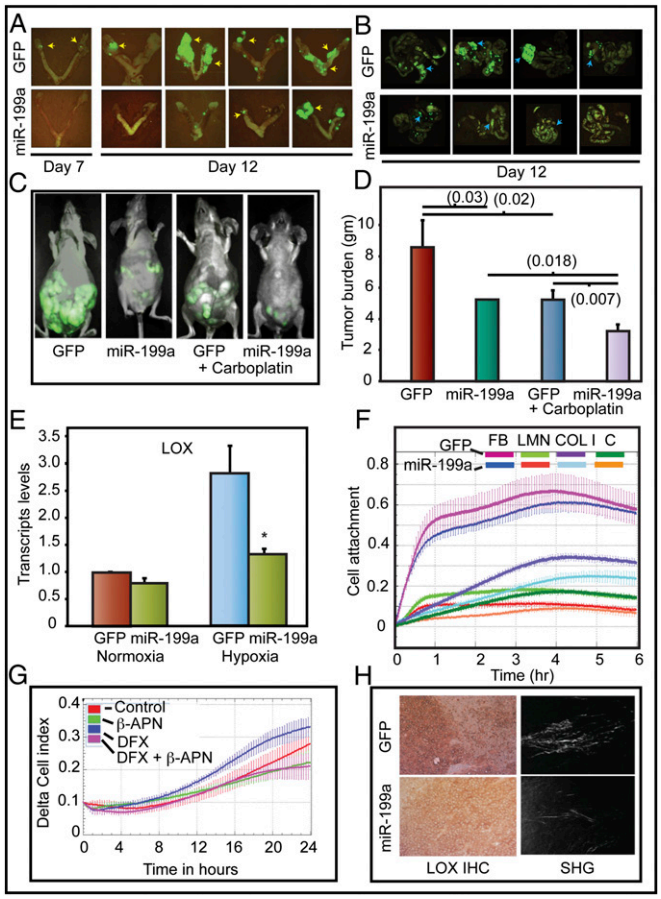


**Fig. 6.** miR-199a inhibits peritoneal seeding and tumor burden. (*A*) Representative images of female athymic mice injected intraperitoneally (i.p.) with A2780 GFP or miR-199a/GFP are shown. (*B*) The yellow arrows show tumor seeding, and the blue arrows show GI metastases. (*C*) Representative images of tumor burden. (*D*) Wet weight of tumors. Values represent mean ± SD. *P* values are shown in parentheses. (*E*) LOX transcript levels were determined by qPCR. Each value is a mean of three independent experiments (**P* < 0.05). (*F*) Real-time cell attachment to ECM components was measured by electrical impedance (cell index). C, control; COL I, collagen type 1; FB, fibronectin; LMN, laminin. (*G*) Effect of LOX inhibitor, β-aminopropionitrile (β-APN) on Transwell migration of cells. DFX, desferrioxamine, 100 μM. (*H*) Control and miR-199a–expressing A2780 tumor sections were stained for LOX [immunohistochemistry (IHC)] and second harmonic generation (SHG) to evaluate collagen deposition. Representative images are shown.

expression via HIF. As a consequence, miR-199a inhibits ovarian cancer cell seeding and metastasis.

**LOX Expression Negatively Correlates with Survival in Ovarian Cancer.** We next compared the expression of LOX with miR-199a in a limited number of tumor sections. LOX was localized by immunohistochemistry and miR-199a by in situ hybridization. Generally, there was a negative correlation between miR-199a expression and LOX immunoreactivity (Fig. 7*A*). For example, OV5 had low levels of miR-199a and highest intensity for LOX staining, whereas higher expression of miR-199a in OV10 sample showed lower LOX staining. However, we could not conclude from this study whether LOX expression had any significance to tumor progression. This led us to investigate the relationship between LOX expression and survival probability in ovarian cancer patients. These analyses showed that progression-free (Fig. 7*B*) and overall survival (Fig. 7*C*) was significantly reduced in the cohort of patients overexpressing LOX.

## Discussion

Endocytosis is one of the cellular functions dampened during hypoxia (3, 4, 12). Endocytosis is a complex energy-consuming cellular process. Earlier studies have shown that HIF-1 down-regulates rababtin-5 and inhibit endosomal fusion leading to deceleration of endocytosis (4). The present studies show that HIF-1 inhibits DNM2, which is involved in endosomal vesicle budding. HIF-1 is widely known to positively regulate transcription of several genes. HIF-1 also down-regulates some target genes such as α-fetoprotein (13) and hepcidin (14). HIF-1–deficient mice show abnormal iron regulation (15). Down-regulation of DNM2 increases HIF-1α and HIF-2α stabilization. Reduced iron could contribute to HIF stabilization. Our studies show that HIF-1 could transcriptionally suppress *DNM2*. DNM2 knockdown with siRNA up-regulated HIF-2α in addition to HIF-1α. Because HIF-2α binds to HRE elements with equal efficiency, it is likely that HIF-2α could coregulate *DNM2* expression. HRE elements are conserved in *DNM* promoters of rodents and zebrafish, raising the possibility of HIF-mediated regulation of DNM across different species.

Our studies further show that miR-199a, which is encoded from the DNM gene opposite strand, is also directly involved in regulating HIF. Micro-RNAs regulate tumor cell migration, angiogenesis, and metastasis (16). Hypoxia is known to induce changes in a number of micro-RNAs (17). Hypoxia down-regulates Dicer and thereby alters microRNA biogenesis. Furthermore, hypoxia-responsive miRNAs regulate argonaute1 (AGO1) and affect miR targeting (18). Our studies suggest that individual micro-RNA could be differentially regulated by transcriptional suppression. Microarray data show that not all micro-RNA are reduced during hypoxia. For example, miR-210 and miR-424 are

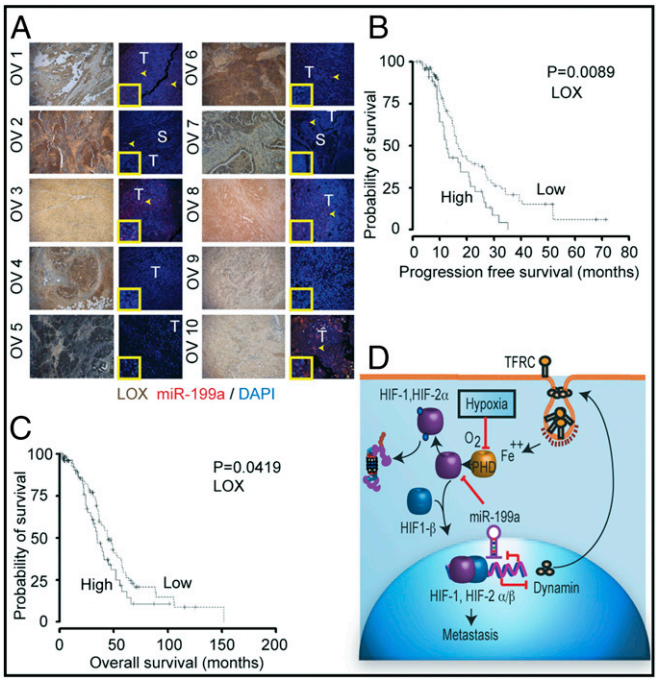


**Fig. 7.** miR-199a expression in tissue samples from EOC patients and LOX expression. (*A*) Representative images of LOX expression and miR-199a in EOC. LOX staining (brown; lanes 1 and 3) and miR-199a in situ hybridization (red; lanes 2 and 4). The arrows indicate areas of miR-199a in situ hybridization. S, stroma; T, tumor. (*Inset*) Magnified area showing hybridization signal. (*B*) Kaplan–Meier plot of EOC patient TCGA data correlating LOX expression to progression-free survival (solid line, high LOX) (dashed line, low LOX). (*C*) Overall survival of ovarian cancer patients as related to LOX expression. (*D*) Schematic diagram showing reciprocal regulation of endocytic pathway (DNM) and HIF through miR-199a.

up-regulated, whereas miR-199a is down-regulated during hypoxia. Changes in miR-199a are at least in part regulated at the transcriptional level. A recent study by Ho et al. (19) showed VHL-dependent down-regulation of Dicer. Dicer-dependent generation of miR-185, was found to target HIF-2α transcripts. In addition, miR-17-92 cluster regulates HIF-1α via c-myc (20). A recent study demonstrated an intricate relationship between miR-20a, HIF-1α, and c-Myc (21). We have identified miR-199a as an important mediator in the regulation of HIF levels in EOCs. Our studies provide evidence for a dual targeting of both HIF-1α and HIF-2α by miR-199a.

miR-199a suppressed both HIF-1α and HIF-2α levels, and has functional consequences in EOCs. miR-199a overexpression in EOCs decreased angiogenesis and increased tumor necrosis (Fig. S7 *A–E*). miR-199a overexpression inhibited EOC attachment to matrix, migration, and in vivo tumor seeding and growth. HIF-mediated changes in matrix/tissue remodeling genes significantly affect the survival of ovarian cancer patients (9). Our studies demonstrate that miR-199a suppresses LOX expression in ovarian cancer cells. LOX is induced by HIF-1, cross-links collagens, and facilitates tumor metastasis (7, 22, 23). Hypoxia affects modification of collagens and metastasis of sarcomas (24). miR-199a also targets IKKβ (25). miR-199a expression, however, did not directly correlate with LOX expression in The Cancer Genome Atlas database. This discordance raises the interesting possibility that HIF-1α 3′-UTR could have been altered during tumor progression, thereby deregulating miR-199a–mediated effects on HIF-1α levels. Mayr and Bartel (26) have shown that 3′-UTRs are shortened in cancer cells to overcome micro-RNA–mediated regulation of oncogenes, and widespread shortening of 3′-UTRs by alternative cleavage and polyadenylation.

Our studies establish a direct link between the DNM2 (endocytic pathway) and HIF regulation. DNM2 and HIF negatively regulate each other. Indeed, *HIF1A* promoter methylation positively correlates with DNM2 expression in ovarian cancer tissues (Fig. S8), indicating a potential HIF-dependent regulation in vivo. miR-199a, arising from the *DNM* gene opposite strand, targets HIF and indirectly affects the tumor microenvironment through LOX. These findings raise the intriguing possibility of modulating intracellular iron levels in ovarian cancer cells to control tumor progression.

## Methods

**Cell Culture and Hypoxia.** Hypoxia was achieved by flushing modular incubator chambers (Billups-Rothenberg) with 95% $N_2$, 5% $CO_2$ for 15 min to effect $O_2$ levels of ∼3% in the media. The mutant P402A/P564A HIF1α (P-to-A HIF1α) was acquired from Addgene [plasmid 18955; contributed by William Kaelin (Dana-Farber Cancer Center, Boston) (27)]. K44A-dynamin 2 constructs were from M. McNiven (Mayo Clinic, Rochester, MN).

**Custom Micro-RNA Microarray.** Custom miRNA microarray experiments and analyses were performed as previously described (10).

Immunoblotting was carried out as per previously published methods (28).

ChIP was carried out as per manufacturer's instructions using ExactaChIP Human/Mouse HIF-1α from R&D Systems in normoxic and hypoxic conditions.

**Knockdown Experiments.** siRNA DNM2 and control duplex were obtained from Qiagen. A2780 cells were transfected with 1.6 μg of siRNA using Lipofectamine (Invitrogen).

**Immunohistochemistry/Immunofluorescence.** Cells were grown in chamber slides, fixed, permeabilized, and then treated with primary antibody. Secondary antibody conjugated to TRITC or Alexa Fluor 647 was used for visualization. Nuclear localization was quantified by NIH Image analysis software.

Scratch wound assays, lentiviral vector construction, transduction, and luciferase assays were carried out as per previously published methods (28).

**Real-Time Cell Migration.** xCELLIgence system from ACEA Biosciences was used. Experiments were carried out according to manufacturer's published methods.

**In Vivo Tumor Models.** Tumor growth studies were carried out as per previously published methods. Details are given in *SI Methods*.

**Statistics.** Statistical significance was determined using one-way ANOVA or the unpaired Student *t* test (one-tailed), depending on the number of experimental groups analyzed.

**ACKNOWLEDGMENTS.** This work was supported in part by grants from the National Institutes of Health (CA114340 and DA031201), the Sparboe Endowment for Women's Cancer Research, and the Interdisciplinary Drug Abuse Research Training Program funded by National Institute on Drug Abuse (T32DA007097). H.P.J. was a trainee of the University of Minnesota Medical Scientist Training Program.

1. Jemal A, et al. (2007) Cancer statistics, 2007. *CA Cancer J Clin* 57(1):43–66.
2. Kim KS, et al. (2006) Hypoxia enhances lysophosphatidic acid responsiveness in ovarian cancer cells and lysophosphatidic acid induces ovarian tumor metastasis in vivo. *Cancer Res* 66(16):7983–7990.
3. Mosesson Y, Mills GB, Yarden Y (2008) Derailed endocytosis: An emerging feature of cancer. *Nat Rev Cancer* 8(11):835–850.
4. Wang Y, et al. (2009) Regulation of endocytosis via the oxygen-sensing pathway. *Nat Med* 15(3):319–324.
5. Semenza GL (2012) Hypoxia-inducible factors: Mediators of cancer progression and targets for cancer therapy. *Trends Pharmacol Sci* 33(4):207–214.
6. Keith B, Johnson RS, Simon MC (2012) HIF1α and HIF2α: Sibling rivalry in hypoxic tumour growth and progression. *Nat Rev Cancer* 12(1):9–22.
7. Schietke R, et al. (2010) The lysyl oxidases LOX and LOXL2 are necessary and sufficient to repress E-cadherin in hypoxia: Insights into cellular transformation processes mediated by HIF-1. *J Biol Chem* 285(9):6658–6669.
8. Seeber LM, et al. (2011) The role of hypoxia inducible factor-1alpha in gynecological cancer. *Crit Rev Oncol Hematol* 78(3):173–184.
9. Markert EK, Levine AJ, Vazquez A (2012) Proliferation and tissue remodeling in cancer: The hallmarks revisited. *Cell Death Dis* 3:e397.
10. Zhang X, Xu W, Tan J, Zeng Y (2009) Stripping custom microRNA microarrays and the lessons learned about probe-slide interactions. *Anal Biochem* 386(2):222–227.
11. Erler JT, et al. (2006) Lysyl oxidase is essential for hypoxia-induced metastasis. *Nature* 440(7088):1222–1226.
12. Joffre C, et al. (2011) A direct role for Met endocytosis in tumorigenesis. *Nat Cell Biol* 13(7):827–837.
13. Mazure NM, et al. (2002) Repression of alpha-fetoprotein gene expression under hypoxic conditions in human hepatoma cells: Characterization of a negative hypoxia response element that mediates opposite effects of hypoxia inducible factor-1 and c-Myc. *Cancer Res* 62(4):1158–1165.
14. Peyssonnaux C, et al. (2007) Regulation of iron homeostasis by the hypoxia-inducible transcription factors (HIFs). *J Clin Invest* 117(7):1926–1932.
15. Yoon D, et al. (2006) Hypoxia-inducible factor-1 deficiency results in dysregulated erythropoiesis signaling and iron homeostasis in mouse development. *J Biol Chem* 281(35):25703–25711.
16. Iorio MV, Croce CM (2012) microRNA involvement in human cancer. *Carcinogenesis* 33(6):1126–1133.
17. Cottrill KA, Chan SY, Loscalzo J (2014) Hypoxamirs and Mitochondrial Metabolism. *Antioxid Redox Signal*, in press.
18. Chen Z, et al. (2013) Hypoxia-responsive miRNAs target argonaute 1 to promote angiogenesis. *J Clin Invest* 123(3):1057–1067.
19. Ho JJ, et al. (2012) Functional importance of Dicer protein in the adaptive cellular response to hypoxia. *J Biol Chem* 287(34):29003–29020.
20. Taguchi A, et al. (2008) Identification of hypoxia-inducible factor-1 alpha as a novel target for miR-17-92 microRNA cluster. *Cancer Res* 68(14):5540–5545.
21. He M, et al. (2013) HIF-1α downregulates miR-17/20a directly targeting p21 and STAT3: A role in myeloid leukemic cell differentiation. *Cell Death Differ* 20(3):408–418.
22. Barker HE, Cox TR, Erler JT (2012) The rationale for targeting the LOX family in cancer. *Nat Rev Cancer* 12(8):540–552.
23. Levental KR, et al. (2009) Matrix crosslinking forces tumor progression by enhancing integrin signaling. *Cell* 139(5):891–906.
24. Eisinger-Mathason TS, et al. (2013) Hypoxia-dependent modification of collagen networks promotes sarcoma metastasis. *Cancer Discov* 3(10):1190–1205.
25. Chen R, et al. (2008) Regulation of IKKbeta by miR-199a affects NF-kappaB activity in ovarian cancer cells. *Oncogene* 27(34):4712–4723.
26. Mayr C, Bartel DP (2009) Widespread shortening of 3′UTRs by alternative cleavage and polyadenylation activates oncogenes in cancer cells. *Cell* 138(4):673–684.
27. Yan Q, Bartz S, Mao M, Li L, Kaelin WG, Jr. (2007) The hypoxia-inducible factor 2alpha N-terminal and C-terminal transactivation domains cooperate to promote renal tumorigenesis in vivo. *Mol Cell Biol* 27(6):2092–2102.
28. Ghosh G, et al. (2010) Hypoxia-induced microRNA-424 expression in human endothelial cells regulates HIF-α isoforms and promotes angiogenesis. *J Clin Invest* 120(11):4141–4154.